24th International Conference on Renewable Energies and Power Quality (ICREPQ'26)
Santander (Spain), 10th to 12th June 2026
E&Q Journal - ISSN:2659-8779. Volume 4. July 2026

Data driven identification and current control on dual active bridge systems for low power applications

Arroyo. Jesus[1], Tafur. Julio[2] and Sal y Rosas. Damian[3]

[1]Control and Automation Engineering Master Degree Program
, Pontificia Universidad Catolica del Peru
Avenida Universitaria 1801, 15082 San Miguel, Lima (Peru). +51931198033, gabriel.arroyop@pucp.edu.pe

[2] Control and Automation Engineering Master Degree Program
, Pontificia Universidad Catolica del Peru
Avenida Universitaria 1801, 15082 San Miguel, Lima (Peru). +51962698622, jtafur@pucp.edu.pe

[3] LAAS-CNRS, University of Toulouse, 31031 Toulouse, France,+51964849200, dsalyrosas@laas.fr

Abstract. This work presents a data-driven methodology for the identification and control of Dual Active Bridge (DAB) DC–DC converters, aimed at reducing the complexity associated with highly nonlinear analytical models. By exploiting an angle phase-shift representation instead of a detailed PWM-based model, the proposed approach simplifies both system excitation and identification while preserving the essential power-transfer dynamics of the converter. A frequency-domain control strategy is subsequently developed based on the identified model, enabling systematic loop-shaping and robust controller design. The resulting discrete-time controller achieves accurate reference tracking and stable regulation in simulation tests, demonstrating that the proposed pipeline provides an effective and practical alternative to conventional model-based control approaches for DAB systems

Key words. System identification, non lineal systems, dual active bridge, data-driven control.

1. Introduction

Modern power conversion systems increasingly demand advanced control solutions capable of ensuring high efficiency, bidirectional power flow, and fast dynamic response under varying operating conditions. In this context, the Dual Active Bridge (DAB) DC–DC converter has emerged as a key topology for isolated power conversion applications due to its inherent bidirectional capability, galvanic isolation, high power density, and flexible control through phase-shift modulation. Foundational research on DAB modeling has established averaged and generalized dynamic representations that enable systematic controller design and stability analysis in closed-loop operation [1].

Building upon these modeling frameworks, several control strategies have been proposed to enhance DAB performance in practical applications. Predictive and model-based control approaches have demonstrated superior transient behavior and robustness compared to classical PI controllers, particularly in DC microgrids and energy storage systems where fast power regulation is required [2]. Furthermore, control formulations that explicitly account for the nonlinear characteristics of the DAB have been shown to improve efficiency and dynamic performance over wide operating ranges [3].

Another significant research direction has focused on modulation and control strategies that guarantee soft-switching operation under varying load and power transfer conditions. Such approaches are essential for reducing switching losses and improving overall system efficiency, especially in high-frequency and high-power applications [4]. However, these strategies typically rely on accurate system models and well-known parameters, which may vary over time due to component aging, temperature changes, and operating point variations.

Despite the extensive literature on model-based control of DAB converters, data-driven identification and control techniques remain relatively underexplored in this domain. Leveraging operational data to identify system dynamics and design control laws offers a promising alternative to purely analytical approaches, with the potential to enhance robustness against parametric uncertainties and modeling errors. Motivated by this gap, this paper investigates a data-driven identification and frequency-domain control methodology applied to dual active bridge systems, with particular emphasis on simplicity, interpretability, and suitability for real-time digital implementation.

2. Methods

Dual Active Bridge modelling and data acquisition

The Dual Active Bridge (DAB) converter is a widely adopted isolated DC–DC topology for medium- and high-power applications due to its bidirectional power flow capability, see Fig.1., galvanic isolation, and high power density. Its operation relies on phase-shift modulation between two full bridges, where the transferred power is primarily controlled by the relative phase angle between the primary and secondary bridge voltages [5], [6].

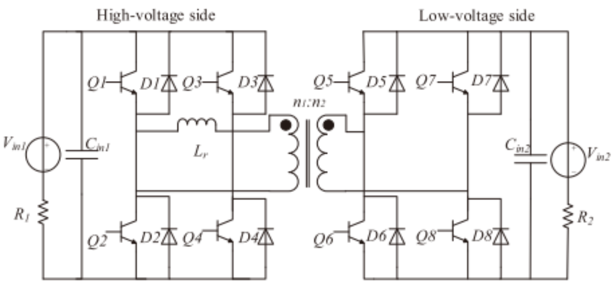

Fig.1. DAB topology. Source: [7]

Despite the existence of detailed analytical models based on averaged or switching descriptions, these models often require accurate knowledge of parasitic parameters, transformer leakage inductance, and switching non-idealities, which are difficult to obtain in practical scenarios. For this reason, a data-driven identification strategy is adopted in this work, treating the DAB system as a black-box dynamic process. In order to make the model more realistic, a Panasonic NCR18650B battery was connected to the secondary of the converter, as a charge station, suitable for power applications, as seen in Fig.2.:

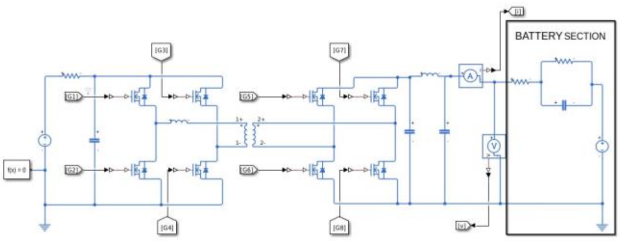

Fig.2. Simulation structure.

Although the proposed methods are initially validated in simulation, all identification and control stages are explicitly designed to be directly transferable to real experimental setups, without relying on inaccessible internal states or idealized assumptions.

Angle injection model and excitation strategy

To simplify the modulation and excitation process, an angle injection model was developed. Instead of directly generating PWM signals for each bridge leg, the DAB is excited through a single control variable: the phase shift angle between the primary and secondary bridges. This abstraction significantly reduces implementation complexity while preserving the essential nonlinear power-transfer behavior of the converter.

The angle injection block consists of the following components, see Fig.3.:

1) *A phase-angle generator defining the relative displacement between bridge voltages.*
2) *A mapping stage translating phase angle into effective bridge modulation commands.*
3) *A limiter ensures safe operating bounds for the injected phase angle.*

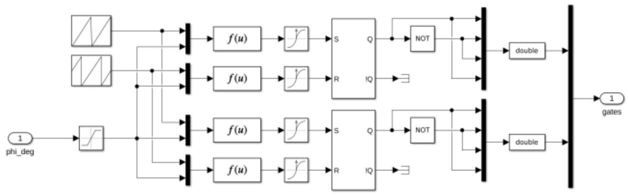

Fig.3. Phase-angle generator block

Frequency sweep and black-box response analysis

Using the angle injection model, a frequency sweep excitation is applied to the DAB system. The injected phase angle is modulated with a pwm signal with a 50% of duty cycle perturbation over a phase angle shift range from -20 to 20 degrees in steps of 0.5 degrees each 10 milliseconds. This approach allows the system to be analyzed as a black-box, without assuming any prior structure of its internal dynamics.

The measured input-output data consists of the angle injected and the current response after a filtering stage, avoiding the system's natural high frequency components, observe Fig.4.:

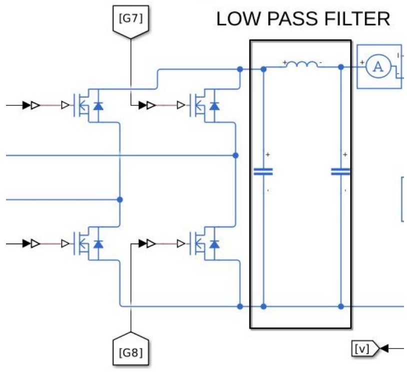

Fig.4. Low-pass filter implemented.

Which leads to first the full sweep between -180 and 180 degrees, with 0.1 degrees of step for better, see Fig.5., Where small high frequency noise can be seen, but not as extreme as without the filter. Which is a nice response for the system and can be used for a precise identification process.

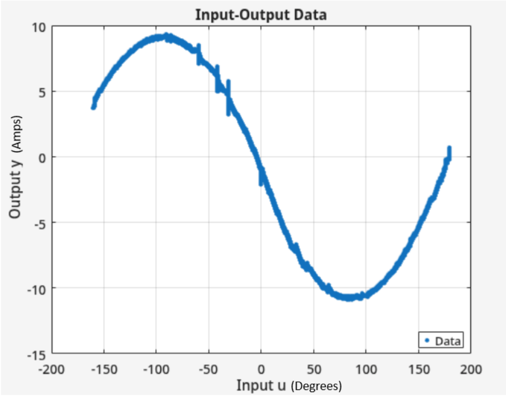

Fig.5. Angle phase shift vs Current filtered obtained data

This response has a fairly good linear area between -50 and 50 degrees, this linear area was extracted with a second experiment and corresponds to Fig.6.:

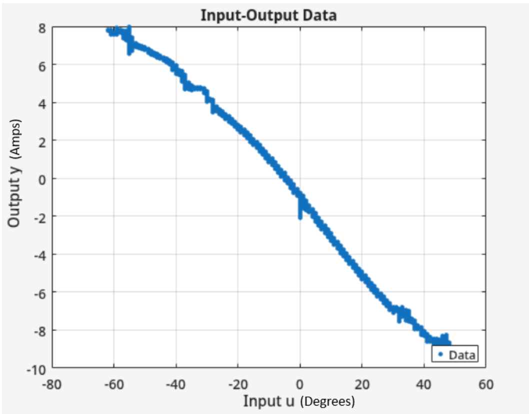

Fig.6. Angle phase shift vs Current linear zone

Therefore, this zone was selected as the operational zone in order to design the control.

Noise reduction and system identification

The raw experimental data inherently contain switching ripple, measurement noise, and nonlinear distortions. To mitigate these effects, an LC low-pass filter was added to the design, see fig.2, with a cut-off frequency of around 1.2kHz, as most of power systems actually work on low frequencies, around 50-60Hz, this filter is ideally fitted according to the equation:

$$f_c = \frac{1}{2\pi\sqrt{LC}} \quad (1)$$

Taking as base a value of 2200µF, the calculated inductance value for L, for 1.2kHz is around 8µH. Thus reducing the noisy original signal which has a lot of high frequency components, therefore leading to the linear zone selected.

After the identification process, using the toolbox from matlab with a non linear least squares algorithm, a first order model with 92.2% of accuracy was obtained, see Fig.7.:

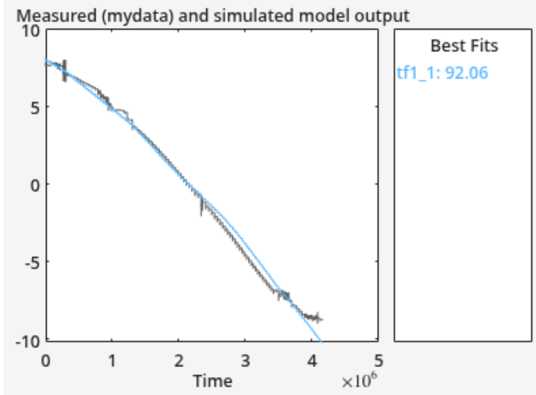

Fig.7. Best fit model.

Which transfer function is:

$$G(s) = \frac{-0.1725s - 2.511 * 10^{-8}}{s + 1.448 * 10^{-17}} \quad (2)$$

Which has physical concordance, since according to [10], the transfer function for an angle-current model is:

$$G_{\phi i}(s) = \frac{\hat{i}_{b2}}{\hat{\phi}} = \frac{d\langle i_{b2}\rangle}{dt} = \frac{NV_1(1-4\Phi)}{f_s L} \quad (3)$$

Which is represented as a static gain.

This model is sufficiently accurate for control design purposes, suitable for real-time embedded implementation.

Discretization and control-oriented representation

Since the ultimate goal of this research is real-time digital control, the identified continuous-time model is discretized using the Tustin (bilinear) transformation, which provides a good compromise between frequency warping and numerical robustness. Regarding the sampling frequency, according to classic control theory, the sampling time should be at least 10 times faster (ideally 20) than the bandwidth of the system. The base switching frequency is 1kHz, this was used to choose the bandwidth of the controlled system. A good bandwidth, according to [11] is the one that could handle all the possible work frequencies and at the same time stay away from the switching frequency, therefore, 250Hz was chosen because of its remoteness from the switching frequency and being in the range of most power systems. So, with the bandwidth properly selected, the sampling time on its most ideal case can be calculated as:

$$T_s \leq \frac{1}{20 * f_{BW}} \quad (4)$$

Where, after doing the calculations, the sampling time should be less or equal to 0.2 milliseconds. So a sampling time of 0.1 milliseconds was selected.

In order to discretize the system, as mentioned earlier the Tustin transformation was used, finally resulting the discrete transfer function as:

$$G(z) = \frac{-0.1725z + 0.1725}{z - 1} \quad (5)$$

And its state-space model:

$$A = [1]$$
$$B = [-1.907 * 10^{-6}]$$
$$C = [-1.31 * 10^{-6}]$$
$$D = [-0.1725] \quad (6)$$

This last model is particularly useful, since it gives information about the controllability of the system, which, being a first order model and observing the state-space is clear that it is fully controllable.

Control design

The control design process begins with the analysis of the discrete-time model in the frequency domain. The Bode diagram of the identified plant is evaluated to assess gain margin, phase margin, resonant modes, and bandwidth limitations. See Fig.8.:

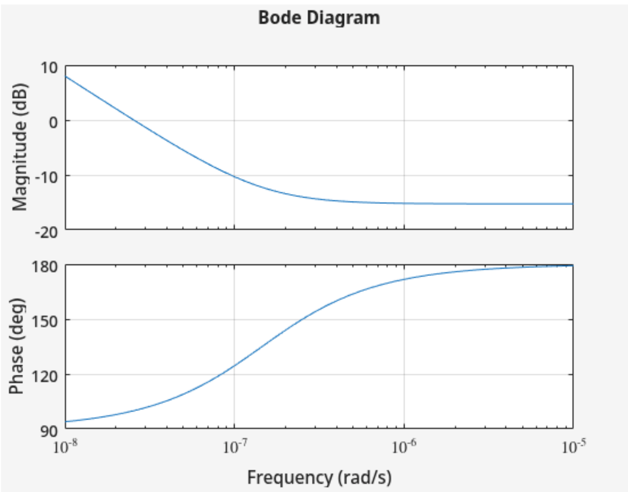

Fig.8. Bode diagram of the system

Based on this analysis, a frequency-domain controller is designed to ensure stability, a prescribed phase margin of 90 degrees, and robust performance against modeling uncertainties and load variations. As observed in the Bode diagram, the plant exhibits a smooth, monotonic magnitude roll-off without resonant peaks and a phase evolution consistent with a predominantly integrative behavior in the linear operating region, which makes it suitable for classical loop-shaping techniques. According to the bandwidth selected, the crossover frequency should be fixed at 1570.8 rad/s, and a classical PI controller is adopted, where the 90 degrees phase margin imposes that:

$$\angle C(j\omega_c) = -tan^{-1}\left(\frac{K_i}{K_p\omega_c}\right), \frac{K_i}{K_p\omega_c} \gg 1 \quad (7)$$

From the plant frequency response, the required controller phase contribution is -90 degrees, see equation (7). According to [12], the phase of a PI controller is defined as:

$$\angle C(j\omega_c) = -tan^{(} - 1)\left(\frac{K_i}{K_p\omega_c}\right), \frac{K_i}{K_p\omega_c} \gg 1 \quad (8)$$

Now, defining:

$$\alpha = \frac{K_i}{K_p\omega_c} \quad (9)$$

The proportional gain is defined as:

$$|K_p| = \frac{|K_i|}{\omega_c\alpha} \quad (10)$$

Finally, solving for (8) and (10), the calculated values for the proportional and integral constants are -0.456 and -9120, respectively, which in closed loop with the plant gives the following results.

3. Results

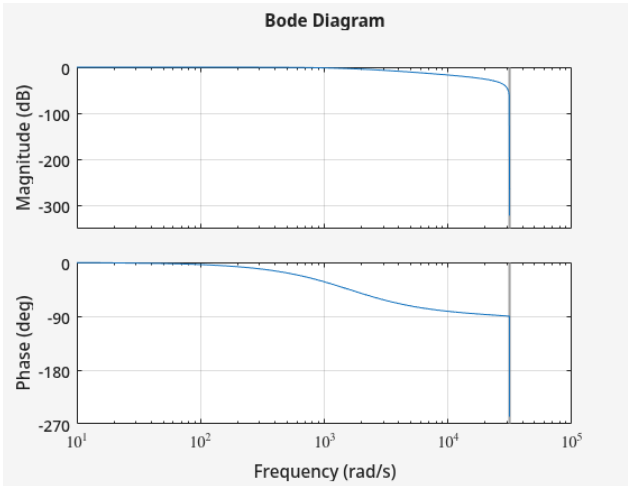

Fig.9.Bode diagram of the system in closed loop with the designed controller.

Fig.9. shows that the controller evidently matches the design criteria. The step response is:

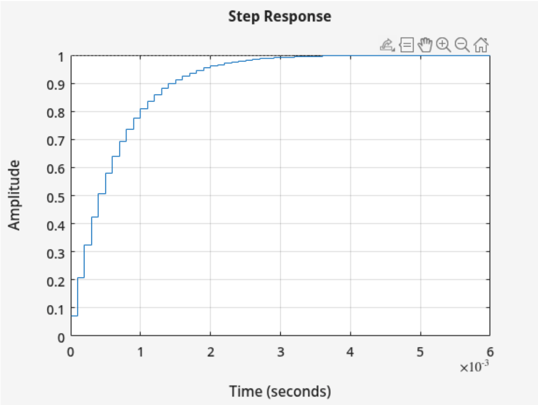

Fig.10.Step response of the closed loop system.

Fig.10. shows that the designed controller is fast and enough for most power systems. The controller was also validated with the system of Fig.2, from where the data was collected, with the following setup:

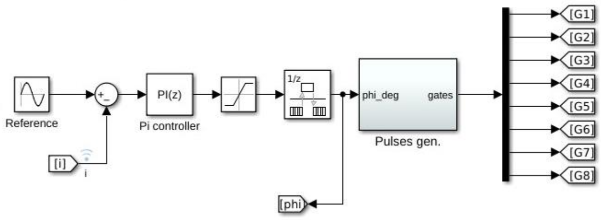

Fig.11.Control setup.

Where a sine wave of amplitude of 1A and frequency of 60Hz was chosen as the reference in order to validate the controller's capability when facing a reference tracking problem, resulting for the current response in Fig.12.:

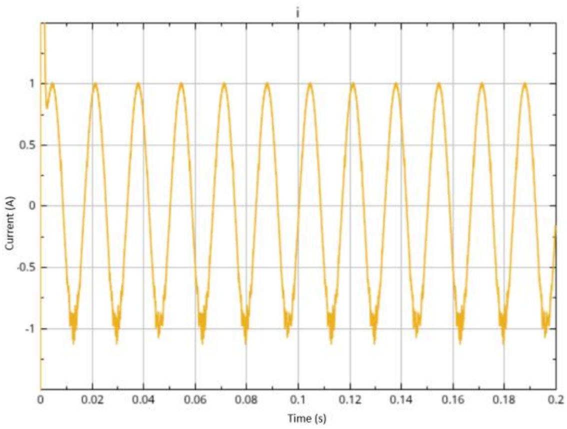

Fig.12.Current response.

And the voltage response in Fig.13.:

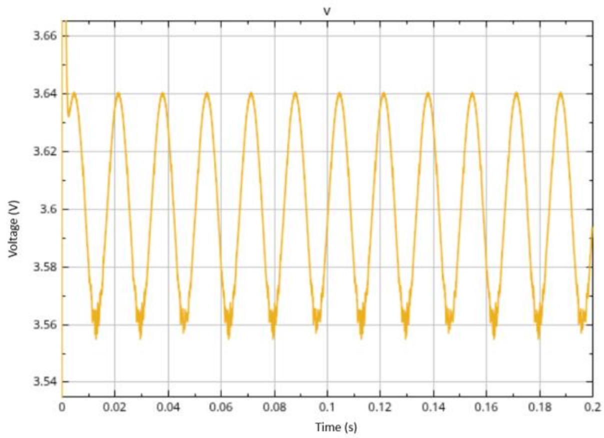

Fig.13.Voltage response.

Where both figures, Fig.12. and Fig.13. show how the controller is able to follow the reference, with a little noise on the bottom edge of the sine wave. This noise is a consequence of the sampling time chosen, which is a little faster than the ideal calculated. Generally it's a good design.

4. Experimental Setup

Since the main objective of this research is to be able to run on real hardware, an experiment was formulated in order to serve as a guide for those interested in following the methods described, a difference equation for the controller was designed, as well as a direct pipeline shown in Fig.14.

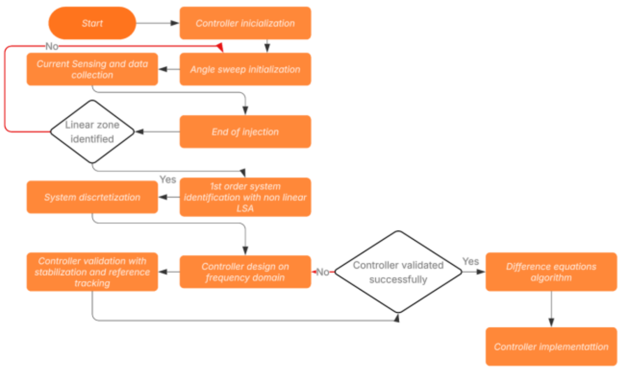

Fig.14. Algorithm pipeline.

For the differences equation, is necessary to start with the PI controller form:

$$K_p + K_i T_s \frac{1}{z-1} \quad (11)$$

From where, omitting the algebraic process, can be implemented as:

$$u[k] = u[k-1] + K_p\left(e[K] - e[K-1]\right) + K_i T_s e[K-1] \quad (12)$$

With the constants calculated from equations (8) and (10):

$$u[k] = u[k-1] - 0.456\left(e[K] - e[K-1]\right) - 0.91 e[K-1] \quad (13)$$

Now equation (13) can be easily implemented on any microcontroller for tests.

5. Conclusions

This paper presented a data-driven identification and control pipeline for Dual Active Bridge DC–DC converters that avoids the complexity associated with highly nonlinear analytical models. By employing an angle phase-shift representation and treating the converter as a black-box system, a compact and accurate linear model was obtained in the relevant operating region. This model enabled the systematic design of a frequency-domain PI controller with prescribed bandwidth and phase margin.

The resulting discrete-time controller demonstrated the ability to accurately track reference signals and maintain stable regulation under test conditions, validating the effectiveness of the proposed methodology. The simplicity of the identification process, together with the robustness of the control design, makes the proposed approach well suited for practical embedded implementations and adaptive power applications. Overall, the results confirm that data-driven techniques provide a viable and efficient alternative for the control of DAB converters in real-world scenarios.

Acknowledgement

This research was supported by Concytec-Prociencia by the Project "Manufactura de Sistemas de Recarga de Baterías de Vehículos eléctricos "Inteligentes", con capacidad de Gestión de Microrredes Eléctricas, y basados sobre principios de Economía Circular" [Contract Nº PE501094745-2025-PROCIENCIA]

References

[1] H. Qin and J. W. Kimball, "Generalized average modeling of dual active bridge DC–DC converter", IEEE Transactions on Power Electronics (2012), Vol. 27, No. 4, pp. 2078–2084.

[2] L. Chen, F. Gao, K. Shen, Z. Wang, L. Tarisciotti, P. Wheeler and T. Dragicevic, "Predictive control based DC microgrid stabilization with the dual active bridge converter", IEEE Transactions on Industrial Electronics (2020), Vol. 67, No. 10, pp. 8944–8956.

[3] F. D. Esteban, "Control of a DC–DC dual active bridge converter in DC microgrids", IEEE Transactions on Industry Applications (2021), Vol. 57, No. 1, pp. 1–9.

[4] G. G. Oggier, G. O. García and A. R. Oliva, "Modulation strategy to operate the dual active bridge DC–DC converter under soft switching in the whole operating range", IEEE Transactions on Power Electronics (2011), Vol. 26, No. 4, pp. 1228–1236.

[5] R. W. De Doncker, D. M. Divan and M. H. Kheraluwala, "A three-phase soft-switched high-power-density DC/DC converter for high-power applications", IEEE Transactions on Industry Applications (1991), Vol. 27, No. 1, pp. 63–73.

[6] F. Krismer and J. W. Kolar, "Accurate small-signal model for the digital control of an automotive bidirectional dual active bridge", IEEE Transactions on Power Electronics (2009), Vol. 24, No. 12, pp. 2756–2768.

[7] X. Li, W. Zhang, W. Chen, Y. Huang and Y. Qiu, "Dual active bridge bidirectional DC–DC converter modeling for battery energy storage system", Proceedings of the 37th Chinese Control Conference (CCC) (2018), Wuhan, China, pp. 1740–1745.

[8] S. Qin, Y. Lei and R. C. N. Pilawa-Podgurski, "Data-driven modeling and control of power converters", IEEE Transactions on Power Electronics (2018), Vol. 33, No. 2, pp. 933–945.

[9] L. Ljung, "System identification: theory for the user", IEEE Control Systems Magazine (2010), Vol. 30, No. 6, pp. 36–38.

[10] S. Shao et al., "Modeling and advanced control of dual-active-bridge DC–DC converters: A review", IEEE Transactions on Power Electronics (2022), Vol. 37, No. 2, pp. 2057–2083.

[11] F. Krismer and J. W. Kolar, "Closed form solution for the optimal efficiency modulation of the dual active bridge converter", IEEE Transactions on Power Electronics (2010), Vol. 25, No. 8, pp. 2086–2099.

[12] K. J. Åström and T. Hägglund, "PID controllers: theory, design, and tuning", Instrument Society of America (ISA) (1995), 2nd Ed.